Cell, Vol. 93, 361–372, May 1, 1998, Copyright ©1998 by Cell Press

Gene Dosage–Dependent Embryonic Development and Proliferation Defects in Mice Lacking the Transcriptional Integrator p300

Tso-Pang Yao,*# Suk P. Oh,† Miriam Fuchs,* Nai-Dong Zhou,* Lian-Ee Ch'ng,* David Newsome,* Roderick T. Bronson,‡ En Li,† David M. Livingston,*‖ and Richard Eckner*§#

*Dana-Farber Cancer Institute and Harvard Medical School
Boston, Massachusetts 02115
†Cardiovascular Research Center
Massachusetts General Hospital and Harvard Medical School
Boston, Massachusetts 02115
‡Department of Pathology
Tufts University Schools of Medicine and Veterinary Medicine
Boston, Massachusetts 02111
§Institute for Molecular Biology
University of Zurich
8057 Zurich
Switzerland

Summary

The transcriptional coactivator and integrator p300 and its closely related family member CBP mediate multiple, signal-dependent transcriptional events. We have generated mice lacking a functional *p300* gene. Animals nullizygous for *p300* died between days 9 and 11.5 of gestation, exhibiting defects in neurulation, cell proliferation, and heart development. Cells derived from p300-deficient embryos displayed specific transcriptional defects and proliferated poorly. Surprisingly, *p300* heterozygotes also manifested considerable embryonic lethality. Moreover, double heterozygosity for *p300* and *cbp* was invariably associated with embryonic death. Thus, mouse development is exquisitely sensitive to the overall gene dosage of *p300* and *cbp*. Our results provide genetic evidence that a coactivator endowed with histone acetyltransferase activity is essential for mammalian cell proliferation and development.

Introduction

p300 and CBP are members of a novel class of transcriptional coactivators that are suspected of being fundamentally important in various signal-modulated transcriptional events. Both proteins interact with a diverse collection of transcription factors that participate in a broad spectrum of biological activities such as cellular differentiation, homeostasis, and growth control (reviewed in Shikama et al., 1997). p300 was originally identified as one of the key cellular proteins targeted by the adenovirus E1A oncoprotein, while CBP was isolated as a protein interacting with the cAMP-responsive transcription factor CREB (Whyte et al., 1989; Chrivia et al., 1993; Eckner et al., 1994). Yet, p300 and CBP are highly related in primary structure (Arany et al., 1994). Moreover, they bind a similar set of cellular target factors and so far appear to carry out comparable functions in biochemical and cotransfection assays (Shikama et al., 1997).

Several protein motifs in p300 and CBP such as a bromodomain, a KIX domain, and three regions rich in Cys/His residues (C/H domains) are well conserved in p300/CBP species ranging from *Drosophila* to *C. elegans* to mammals (Arany et al., 1994; Eckner et al., 1994; Parker et al., 1996; Akimaru et al., 1997). These domains serve as binding sites for sequence-specific transcription factors and other components regulating gene expression. For example, mediated by one of the conserved C/H domains, p300 and CBP can interact with RNA helicase A, which in turn binds RNA polymerase II (Nakajima et al., 1997a). Recruitment of the RNA polymerase II holoenzyme by p300/CBP appears to be an essential step in the process of transcriptional activation by CREB (Nakajima et al., 1997b). p300 and CBP can also recruit other coactivators such as SRC-1, p/CIP, ACTR, and P/CAF (a histone acetylase) to form a larger coactivator complex, which appears to participate in nuclear hormone receptor signaling (Smith et al., 1996; Yang et al., 1996; Yao et al., 1996; Chen et al., 1997; Torchia et al., 1997).

The ability of p300 and CBP to interact with multiple, signal-dependent transcription factors has led to the proposal that these coactivators function as signal integrators by coordinating complex signal transduction events at the transcriptional level (Eckner et al., 1996a; Hanstein et al., 1996; Kamei et al., 1996; Oelgeschlager et al., 1996; Yao et al., 1996). Depending on the context, specific transcription factors can either cooperate or interfere with each other. For example, during skeletal muscle cell differentiation, MyoD and MEF2 family members cooperate to activate synergistically the differentiation program (Molkentin et al., 1995). In vivo, p300 and CBP bind to members of both families and are required for the activity of MyoD and MEF2 proteins (Eckner et al., 1996a; Sartorelli et al., 1997). On the other hand, transcriptional repression among certain transcription factors also appears to be mediated by p300 and CBP. On the collagenase promoter, members of the nuclear receptor and AP-1 families strongly interfere with each other, a phenomenon termed cross-coupling (Reviewed in Schule and Evans, 1991). Both types of transcription factors bind p300 and CBP, and it has been suggested that repression results from competition for limiting amounts of intracellular p300 and CBP (Kamei et al., 1996). These results suggest a complex mode of action for p300 and CBP in coordinating gene expression with signal transduction pathways.

In keeping with this notion, there are likely several mechanisms by which p300 contributes to transcription control. For example, p300 and CBP both express a potent histone acetyltransferase activity (HAT) (Bannister and Kouzarides, 1996; Ogryzko et al., 1996). In vitro, p300 can acetylate the amino-terminal tails of all four

‖To whom correspondence should be addressed.
#These authors contributed equally to this work.

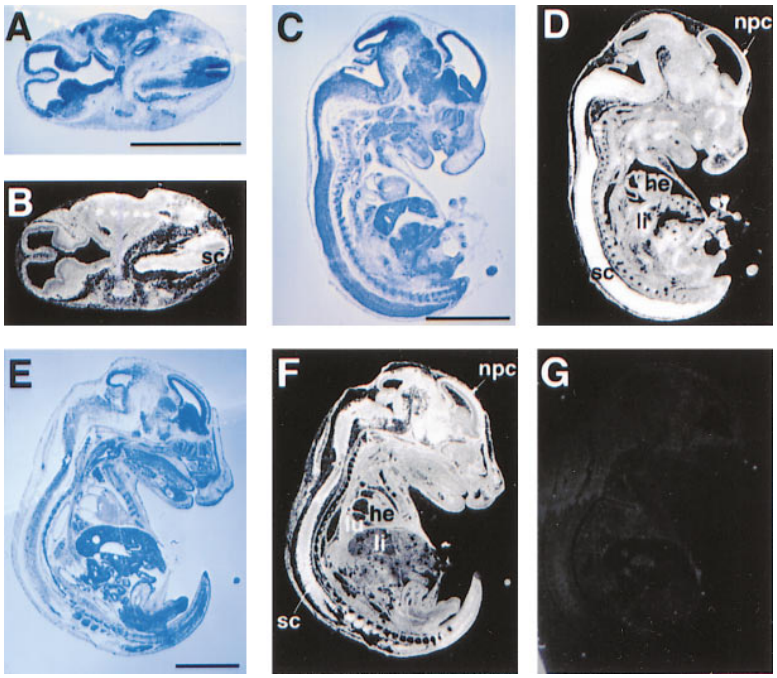

Figure 1. In Situ Analysis of *p300* mRNA Transcript Expression in Mouse Embryogenesis

Dark-field micrographs of a transverse section in the cranial region of an E12.5 (B) and of parasagittal sections of E14.5 (D) and E16.5 (F) mouse embryos are presented after hybridization with a ^{35}S-α-ATP-labeled p300-specific mouse antisense probe. Bright-field micrographs of toluidine blue–stained sections are shown in (A), (C), and (E). Note the widespread expression of *p300* with elevated levels in the central nervous system. Note also the absence of specific signals when a parallel section of the E16.5 embryo in (F) was hybridized with the respective control sense probe (G). Abbreviations: sc, spinal cord; npc, neopallial cortex; lu, lung; li, liver; he, heart. Scale bar = 3 mm.

core histones. Since histone acetylation is known to be increased in transcriptionally active chromatin (Grunstein, 1997; Wade et al., 1997), it is possible that p300/CBP in part facilitates transcription by directly modifying chromatin structure.

Several lines of evidence indicate that deregulation of p300 and CBP activity can cause cellular transformation. Together with members of the retinoblastoma tumor suppresser (pRB) protein family, p300 and CBP constitute the two major cellular targets of the viral oncoprotein E1A and large T antigen (Whyte et al., 1989; Eckner et al., 1996b). Binding of p300/CBP by E1A stimulates quiescent primary cells to proliferate and contributes to ras-mediated cellular transformation (Howe et al., 1990; reviewed in Moran, 1993). By analogy to pRB, which is inactivated upon E1A binding (Nevins, 1992), it is assumed that E1A inactivates growth suppressing functions of p300 and CBP. In keeping with this view, p300 and/or CBP can function as coactivators of p53 in the induction of cell cycle arrest and apoptosis. These functions of p300/CBP are abrogated by E1A (Avantaggiati et al., 1997; Gu et al., 1997; Lill et al., 1997). Interestingly, by acetylating p53, p300 and CBP can also up-regulate the DNA binding activity of p53 (Gu and Roeder, 1997). Another type of deregulation of p300 and CBP activities occurs in some leukemias, where specific chromosomal translocations fuse *p300* or *cbp* to partner genes (Borrow et al., 1996; Ida et al., 1997; Sobulo et al., 1997). The resulting fusion proteins likely exert oncogenic activity, at least in part, by derailing the normal functions of p300/CBP.

The necessity for correct regulation of p300 and CBP family members to prevent human disease is underscored by the recent finding that *cbp* is mutated in Rubinstein Taybi syndrome (RTS, Petrij et al., 1995), a genetic disease characterized by multiple developmental defects and severe mental retardation. Interestingly, affected individuals are heterozygous at the *cbp* locus, suggesting that the dose of the *cbp* gene is critically important in humans.

To investigate the function of p300 and CBP during mouse development, we have disrupted both *p300* and *cbp* genes. In this report we will present the analysis of *p300* mutant animals. Animals lacking both *p300* alleles died around mid-gestation despite the presence of normal quantities of highly homologous CBP. These embryos showed pleiotropic defects in morphogenesis and cell differentiation and, unexpectedly, in proliferation. In keeping with the latter defect, fibroblasts derived from homozygous embryos also manifested a severe deficiency in proliferation. Remarkably, there was also significant embryonic lethality of mice lacking just one copy of *p300*. Compound heterozygous mutants for *p300* and *cbp* invariably died in utero, demonstrating an absolute requirement for a certain combined level of these two closely related proteins for normal animal development. These results establish an essential gene dosage–sensitive role for a mammalian coactivator/histone acetyltransferase in embryogenesis, differentiation, and cell proliferation.

Results

p300 Expression in Mouse Embryogenesis

Analysis of the expression pattern of a gene during mouse development can provide valuable insights regarding its function. As a prelude to disrupting the gene for p300, we have analyzed the distribution of its messenger RNA at different stages of embryogenesis by in situ hybridization. The transcript of *p300* can be detected as early as E7.5 (data not shown) and subsequently in all the developmental stages that we have examined (Figure 1). For the most part, *p300* transcripts appear to be generally expressed in embryos, with an elevated abundance in neural tissues. The almost ubiquitous expression of p300 indicates that this protein

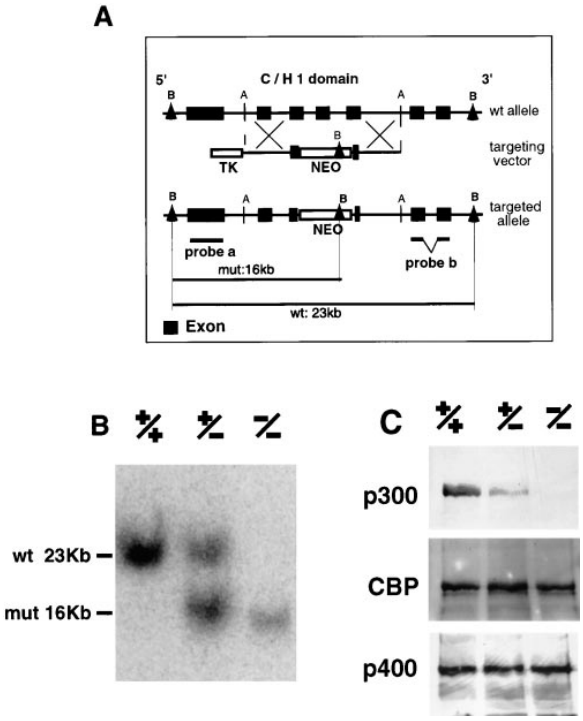

Figure 2. Disruption of the *p300* Gene in Mice

(A) Schematic drawing of the targeting vector. The configuration of the wild-type (wt) allele is shown at the top. In the targeting vector (middle), exons encoding the first Cys/His domain (C/H 1) are replaced by a neomycin resistance gene cassette. The thymidine kinase (*tk*) gene was used for negative selection. The structure of the targeted allele is shown at the bottom. The location of the two external probes (a and b) used to confirm correct targeting events and the size of the diagnostic restriction fragments for probe a (used for the Southern blot in [B]) are indicated. Abbreviations: A, Asp-718; B, BamH1.

(B) Southern blot analysis of genomic DNAs isolated from the yolk sacs of embryos derived from heterozygous parents. The DNA was digested with BamH1 and detected by hybridization to probe a. The wild-type allele is 23 kb in length and the mutant allele is 16 kb.

(C) Western blot analysis of p300, CBP, and p400 protein levels in fibroblast extracts derived from E10.5 embryos. Equivalent amounts (100 μg) of whole cell extract from embryonic fibroblasts were probed with a p300 (RW128) or a CBP (AC26) specific antibody or an antibody (RW144) that recognizes a putative family member, p400. Compared with wild-type cells, p300 protein levels are reduced in +/− cells. No p300 was detected in −/− cells. The expression of the p300 family member CBP (middle panel) and of p400 (bottom) were comparable in all three genotypes.

does not act in a tissue-restricted manner and is consistent with previous work suggesting that p300 is present in all tissue culture cell lines examined (unpublished data).

p300 Gene Targeting

To study the functional importance of p300 in embryogenesis and other signal transduction events, we inactivated the murine *p300* gene. Exons encoding the first Cys/His-rich domain, which is located near the N terminus of p300, were replaced with a PGK-*neo* gene cassette by homologous recombination (Figure 2A). Correctly targeted clones were identified by Southern analysis (Figure 2B). Two different $p300^{+/-}$ ES cell clones were independently injected into blastocysts and gave rise to germline-transmitting chimeric mice that were used to breed homozygous mutant progeny. To test for the generation of true null mutants, the p300 protein level was analyzed by standardized Western blotting in primary fibroblasts derived from embryos of all three genotypes. As expected, the p300 protein level was reduced in +/− and not detected in −/− cells, while those of CBP and a putative family member, p400, were unperturbed and not up-regulated in all three genotypes (Figure 2C). Similar results were obtained using specific immunostaining as the assay (data not shown). These results demonstrate the specificity of the relevant targeting events.

Table 1. Survival of the Progeny of *p300* +/+, +/−, and −/− Mice at Weaning and during Embryogenesis

	Genotype				
	+/+		+/−		−/−
129/Sv	155		132		0
	1	:	0.85		
129 × BL6	149		181		0
	1	:	1.21		
E9.5	13		31		10(2)
	1	:	2.38	:	0.77
E10.5	55(1)		95(6)		47(20)
	1	:	1.64	:	0.85

The top panel gives for each genotype of two different genetic backgrounds (129/Sv and 129/Sv × BL6) the number of viable offspring derived from matings of animals heterozygous for *p300*. The genotyping was carried out at weaning. The lower panel shows the number of live embryos in relation to the three genotypes at E9.5 and E10.5, respectively. The number of dead embryos are indicated in parentheses. The data in the bottom panel is taken from mice with a 129/Sv × BL6 background.

Embryonic Lethality in *p300* Hetero- and Homozygous Mice

To examine the potential influence of genetic background, *p300*-targeted mice were crossed into either an inbred (129/Sv) or heterologous (C57BL/6) background. In both cases, fertile heterozygous animals were born and bred further. Genotyping of offspring from matings of heterozygous animals revealed that the homozygous *p300* mutation results in embryonic lethality (Table 1). In addition, heterozygous mutant mice were underrepresented among weaned pups (Table 1). This phenomenon was initially seen in both genetic backgrounds but was persistently and particularly prominent in the 129/Sv inbred background in which 55% fewer heterozygotes were observed than expected assuming normal Mendelian inheritance. Since no neonatal lethality was seen, a fraction of the heterozygous embryos must have died in utero. Indeed, a small number of +/− mutants were found dead as early as at E10.5 (Table 1, bottom panel). We noted that the more the heterologous 129 × BL6 mice were bred against C57BL/6 mice, the less lethality among *p300* heterozygous animals was observed (see below, Table 2). This indicates that there is a modifier gene(s) in BL6 mice that suppresses the lethality of the $p300^{+/-}$ state.

Table 2. Viability of the Progeny of Matings between *p300*$^{+/-}$ and *cbp*$^{+/-}$ Mice at Weaning

	Genotype			
	p300; CBP +/+; +/+	p300; CBP +/−; +/+	p300; CBP +/+; +/−	p300; CBP +/−; +/−
Number	27	26	17	0
Observed ratio	1	0.96	0.62	0
Expected ratio	1	1	1	1

Mice heterozygous for either *p300* or *cbp* were mated, and the number and genotype of viable offspring was determined at weaning. Note the absence of viable double heterozygous mice (*p300*$^{+/-}$/*cbp*$^{+/-}$). For these experiments, mice with a mixed 129 × BL6 background were used, in which *p300*$^{+/-}$ animals are no longer underrepresented.

In both genetic backgrounds, no *p300* nullizygous embryos could be retrieved past E11.5. In the 129 × BL6 mixed background, most *p300*$^{-/-}$ embryos were still alive at E8.5 and E9.5 (Table 1, bottom panel; data not shown). However, morphologically, *p300*$^{-/-}$ embryos could be distinguished from their wild-type littermates as early as at E8.5, and the defect became more obvious at E9.5 (data not shown). At E10.5, 50% of the −/− embryos were already dead as judged by either absence of obvious heart beating or the presence of signs of reabsorption (Table 1, bottom panel). The *p300*$^{-/-}$ embryos dissected at E10.5 were much smaller than their wild-type littermates and were developmentally retarded (Figure 3A). Frequently, the most severe but still viable mutant embryos had not completed an embryonic process referred to as "turning" (Figure 3A) and contained 12–16 somites, indicating developmental arrest at ~E8.5–E9.0.

In general, *p300*$^{-/-}$ 129 × BL6 embryos tended to arrest a day or so later than 129/Sv embryos. A few of the 129 × BL6 embryos survived beyond E10.5. These embryos displayed a less-disordered phenotype and reached E11.5, after which they died. These late-arresting *p300*$^{-/-}$ 129 × BL6 embryos were again smaller than their wild-type littermates but displayed no gross patterning abnormalities (Figure 3B). However, they exhibited a severe open neural tube defect (NTD). Normally, the neural tube begins to close at E8.5 and completes closure by E9.5. However, in all *p300*$^{-/-}$ mutants and some +/− embryos (see below), neural tube closure was defective. Eventually, various degrees of exencephaly were observed in all *p300* nullizygous embryos (Figures 3A and 3B). Typically, the neural tube failed to fuse from hindbrain to the forebrain region (Figure 3B) or remained completely open in the most severely affected mutants (Figure 3A). The heterogeneity in the severity of *p300* mutants, at least in the 129 × BL6 background, indicates a partial penetrance of the phenotypes possibly due to the existence of genetic modifiers.

Remarkably, in both 129 × BL6 and 129/Sv mice, a significant number of +/− embryos also revealed exencephaly. It was calculated that 6% of 129 × BL6 (6 out of 101 E10.5 +/− embryos analyzed) and 19% of 129/Sv (16 out of 79) +/− embryos displayed this phenotype. The exencephaly was generally restricted to the cranial region and had a different morphological appearance from that present in the −/− mutants (compare Figure 3C with 3B). Specifically, the neural tube defect of +/− embryos was confined to the anterior part of the hindbrain and the midbrain, with the rest of the neural tube fused normally. This partial penetrance of exencephaly is compatible with the restricted lethality observed among +/− embryos (see Table 1).

Examination of histological sections prepared from the cranial area revealed, on the ventral side, collapse of the lumen of the telencephalic vesicles, which may be due to the loss of hydrostatic pressure secondary to the open neural tube defect. On the dorsal side, exencephaly caused by the failure of neural tube closure can be seen (compare Figures 3D and 3E). Abnormalities were also apparent in more rostral areas where neural tissue of unknown origin filled the ventricle, which is normally filled with fluid (marked with an asterisk in Figure 3F). Moreover, the density of mesenchymal cells was lower in the homozygous mutant embryos (compare Figures 3H and 3I), suggesting the possibility of a proliferation defect in those cells (see below). Consistent with the difference in exencephaly morphology, a histological analysis of +/− embryos (Figure 3G) revealed a more advanced, yet incomplete, closure of the neural folds in the hindbrain region than in the corresponding region of −/− embryos (compare Figures 3G and 3E), indicating a milder morphogenetic defect of the neural tissue in +/− than in −/− embryos. Moreover, the neural tube of many of the p300 −/− embryos also had a kinked shape instead of a straight one, and the somites appeared to be less organized (compare Figures 3J and 3K). These results suggest a dosage-dependent role of p300 in the processes of neural tube closure.

Abnormal Heart Development

Because neural tube defects generally do not result in early embryonic lethality, we sought to determine if other developmental abnormalities can be seen in *p300* mutant embryos. We noticed that at E10.5, ~20% of the homozygous mutants showed an enlarged heart cavity and the yolk sac was often poorly vascularized (Figure 4A). Upon closer examination, mutant embryos displayed a severe pericardial effusion (Figure 4B), a clear sign for a dysfunctional embryonic heart. Although no overt patterning defect was visible, detailed histological inspection revealed that ventricular chambers of mutant embryos exhibited significantly reduced trabeculation compared to matched wild-type littermates (compare Figures 4C and 4D). On a functional level, we observed that heart contractions in mutant embryos appeared to be weaker and less extensive than in wild-type embryos. To assess the status of cardiac myocyte differentiation, we analyzed the expression of two cardiac muscle structural proteins, myosin heavy chain (MHC) and α-actinin, in mutant and wild-type E9.5 embryos. Expression levels of MHC (Figures 4E and 4F) or α-actinin (data not shown) were significantly lower in cardiac tissue of mutant compared to wild-type embryos. Taken together, the above results indicate that heart development is perturbed in embryos lacking p300 and raise the possibility that failure of the cardiovascular system may, at least in part, be responsible for the observed embryonic lethality.

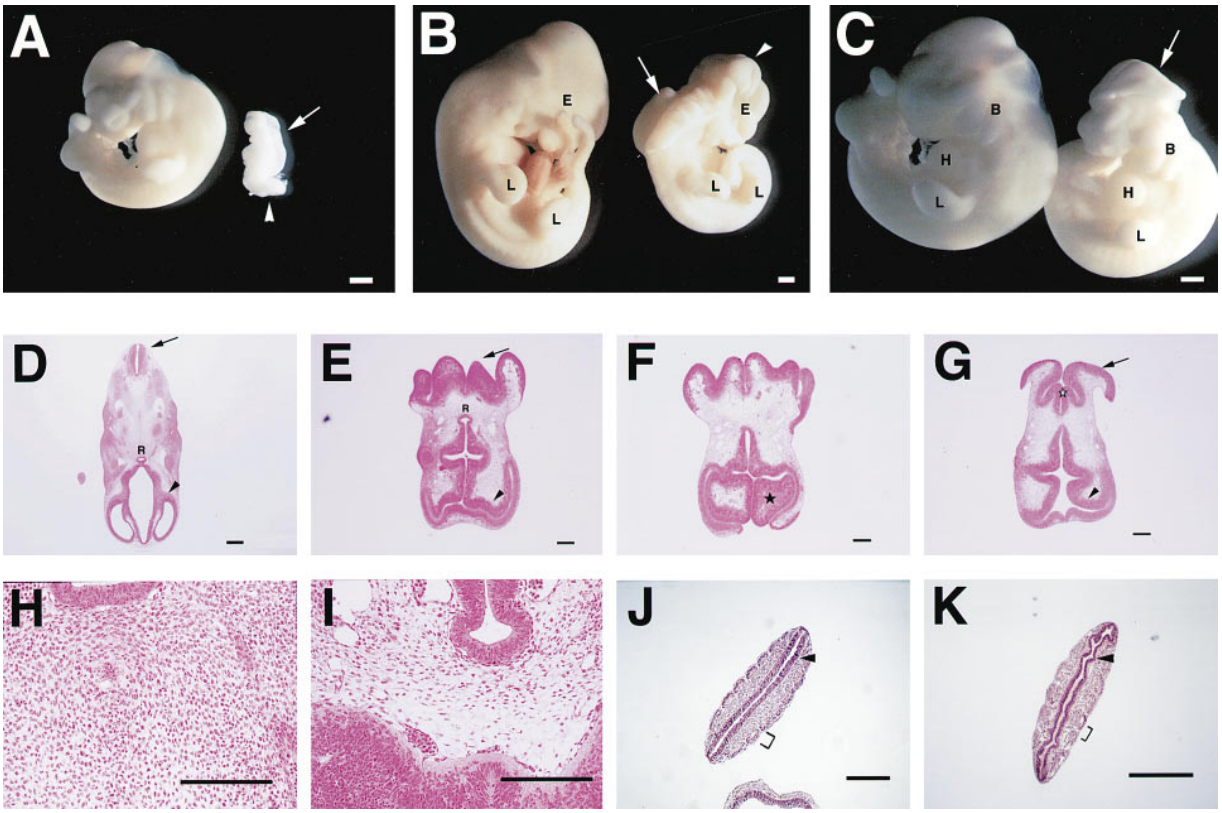

Figure 3. *p300* −/− and a Fraction of +/− Mutants are Developmentally Retarded and Show Defects in Neurulation

A comparison of mutant (−/− or +/−) and control (+/+) embryos by whole-mount (A–C) or by histological analysis (D–K).

(A) A severe −/− mutant (right) and a wild-type littermate (left) isolated at E10.5 are shown. The −/− embryo is much smaller than the +/+ embryo, and it has not completed the process of turning as is evident in the tail region (arrow head). The neural tube (arrow) is open along its full length.

(B) A less-dramatically affected −/− mutant (right) and a wild-type littermate (left) at E11.5 are shown. In the mutant embryo, the neural tube is completely open in the cranial region; however, it is fused in the spinal region. Obvious exencephaly can be observed in the hindbrain (arrow) and the rest of cranial region as well (arrowhead). The eye (E) is smaller in the mutant, and the facial structure appears to be collapsed. Note that both limb buds (L) appear to be normal in the mutant embryos.

(C) A $p300^{+/-}$ mutant (right) with exencephaly and a wild-type littermate (left) at E10.5 are shown. This heterozygous embryo displays symmetrical exencephaly mostly in the midbrain and part of the hindbrain region (arrow). The morphology of exencephaly shown by +/− embryos is distinct from that of a −/− mutant (B). Note that +/− embryos with exencephaly were always somewhat smaller than control +/+ littermates. B, branchial arch; H, heart.

(D–G) Transverse sections through the hindbrain and forebrain of E11.5 wild-type (D), −/− (E and F), and +/− mutant (E10.5) embryos. Both −/− (E) and +/− (G) mutants show exencephaly in the hindbrain region. However, the patterns of exencephaly are different in these two embryos (open asterisk in G). The neural lumen (ventricle) is collapsed in both the −/− and +/− mutants (arrowheads in [D], [E], and [G]). In a more rostral section, an abnormal mass of neural tissue (filled asterisk) was regularly observed in −/− embryos (e.g., in [F]). R, Rathke's pouch.

(H and I) Representations of (D) and (E) at higher magnifications. The density of mesenchymal cells is much reduced in the −/− embryo (I) compared to the wild-type embryo (H)

(J–K) Frontal sections of E10.5 embryos. The neural tube of the −/− animal often had a kinked morphology (arrow in [K]) in contrast to a straight one that was always observed in wild type (J). The somites of the −/− often appeared to be disorganized as well (brackets in [J] and [K]).

Scale bars = 1 mm (A–C, J, K); 0.5mm (D–K).

p300 Is Required for Normal Cell Proliferation

As shown above, embryos lacking p300 were always significantly smaller than their wild-type littermates. One explanation for this difference may be that cell proliferation is reduced in $p300^{-/-}$ embryos. To determine the fraction of cells actively synthesizing DNA, 5-bromo-2′-deoxy-uridine (BrdU) incorporation was assessed. Figure 5 shows sections derived from the upper-trunk region of homozygous E9.5 mutant and wild-type embryos. Nuclei in S-phase are labeled red. Significantly fewer labeled nuclei were detected in sections derived from $p300^{-/-}$ embryos (Figure 5B) compared to those derived from wild-type embryos (Figure 5A) in the mesenchymal and/or neural crest cells surrounding the neural tube. Under higher magnification, it was also clear that BrdU incorporation was much more uniform and intense in the wild-type cells (compare Figures 5C and 5D).

To demonstrate that the proliferation defect observed in animals is cell autonomous rather than a complete secondary defect, fibroblasts derived from *p300* mutant

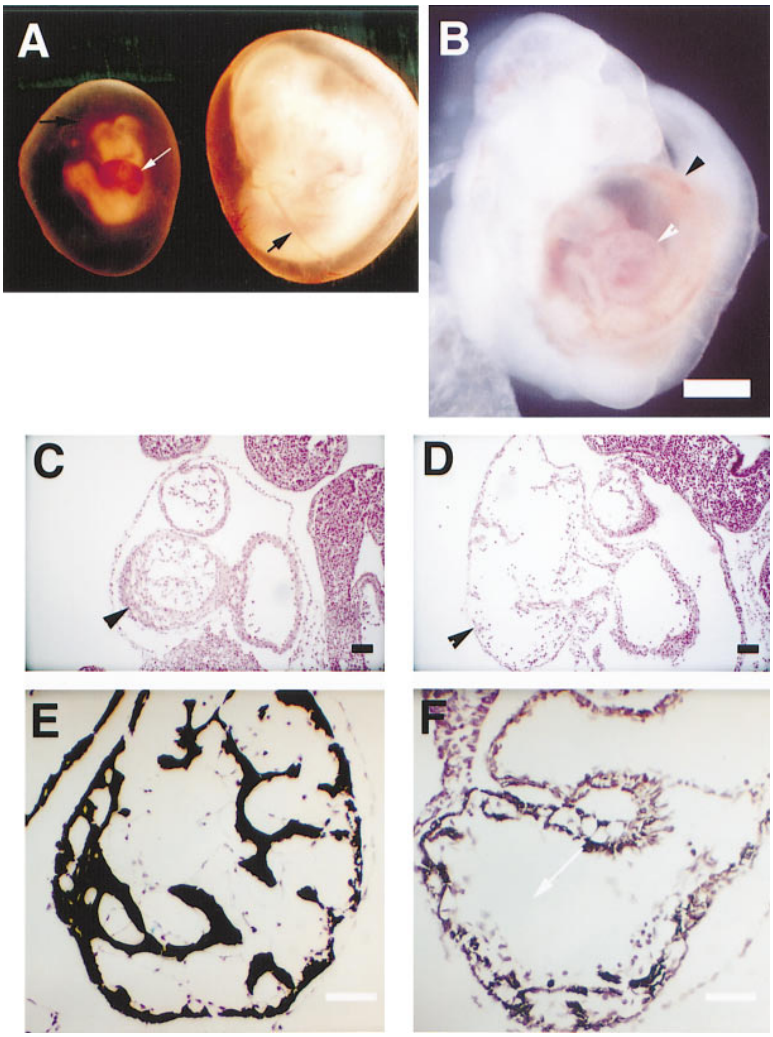

Figure 4. Cardiac Development in $p300^{-/-}$ Mutants

(A) A $p300^{-/-}$ embryo (left) and a wild-type littermate (right), both still contained in their yolk sacs, are shown at E10.5. The mutant embryo displayed an enlarged heart (open arrow), and the yolk sac was poorly vascularized when compared to that of a control littermate (filled arrow).

(B) A higher magnification of an E10.5 $-/-$ embryo with an enlarged heart and a severe pericardial effusion. Note the abnormally enlarged space between the pericardial membrane (filled arrowhead) and the heart itself (open arrow).

(C and D) A frontal section of the E10.5 mutant heart (D) reveals much less extensive trabeculation (arrows) compared with that of a control littermate (C).

(E and F) A transverse section of E9.5 embryos stained with antibody to the cardiac muscle structural protein MHC. The staining is much lower in the mutant heart (F) than in the wild type (E). Note that cardiac trabeculation (arrowhead) is also much more extensive in the wild-type heart.

Scale bars = 1 mm (B) and 0.1 mm (C–F).

and wild-type animals were isolated and their growth curves were determined. Repeatedly, $p300^{-/-}$ cells grew much more slowly than $p300^{+/-}$ or $p300^{+/+}$ MEFs, which appear to have proliferated at a comparable rate (Figure 5E). Furthermore, unlike the heterozygous and wild-type cells, $p300^{-/-}$ cells stopped dividing after three to four cell generations (data not shown). These results demonstrate a major cell proliferation and lifespan defect associated with p300 deficient cells.

Impaired Activity of the Retinoic Acid Receptor in p300 $-/-$ MEFs

The results of numerous studies suggest that p300 and/or CBP act as transcriptional coactivators for several members of the nuclear receptor superfamily. The availability of cells lacking p300 allowed us to investigate receptor activity in a defined genetic background. To this end, wild-type and $p300^{-/-}$ MEFs were transfected with an RAR-responsive reporter gene, and the response to retinoic acid was examined. As shown in Figure 6A, RAR activity was significantly compromised at all RA concentrations tested. Similar results were obtained when a chimeric protein containing the Gal4 DNA binding domain fused to the RAR ligand binding domain was used to activate a reporter gene containing multiple Gal4 sites in its promoter (Figure 6B). By contrast, the activity of the transcription factor CREB stimulated by protein kinase A was comparable in *p300* $-/-$ and $+/+$ cells (Figure 6C). Taken together, these results lend support to the notion that p300 indeed functions as a critical RAR cofactor. On the other hand, in the context of this assay, p300 does not appear to be critical for CREB-dependent gene activity.

Embryonic Lethality of p300 and CBP Compound Heterozygous Animals

To further study the role of p300 and CBP in mouse embryogenesis, we also generated mice lacking CBP. Similar to *p300* mutants, animals homozygous for the disrupted *cbp* allele showed complete embryonic lethality. They also displayed open neural tube defects similar to those seen in $p300^{-/-}$ embryos (Figure 7A; a detailed description of CBP mutants will be presented elsewhere). To generate double heterozygous *p300/cbp* knockout mice, we mated animals heterozygous for *p300* and *cbp*. Surprisingly, no viable compound heterozygous mutants were detected at the time of weaning

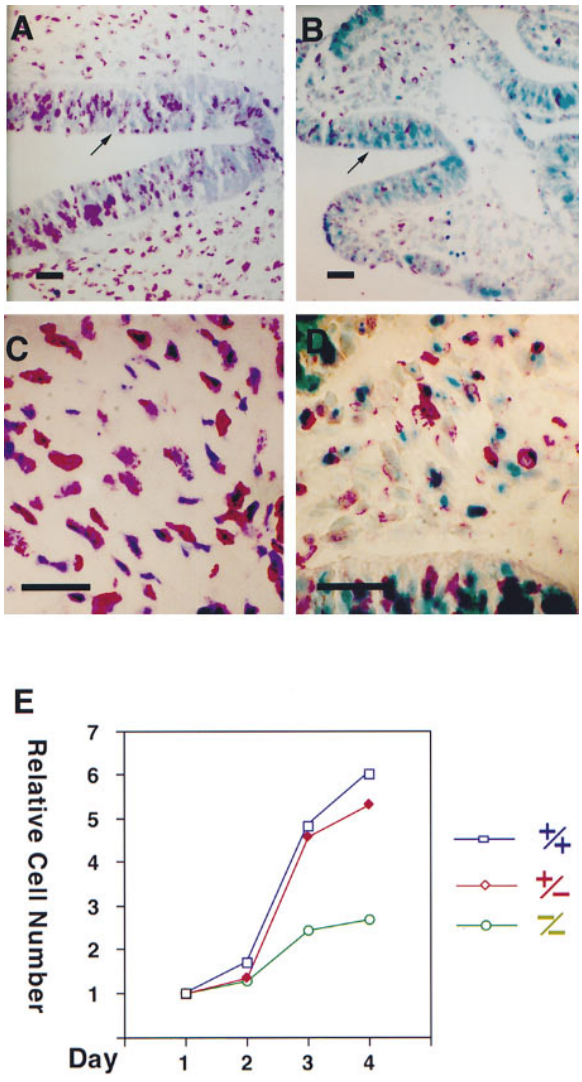

Figure 5. p300-Deficient Embryos and Cells Show Growth Defects

(A–D) Transverse sections of E9.5 embryos were stained with a BrdU-specific antibody. The embryos were pulse-labeled with BrdU for 1.5 hr in utero. The $p300^{-/-}$ embryo (B) had many fewer BrdU-positive cells (red) than its wild-type littermate (A). (C) and (D) are higher magnification images of (A) and (B), respectively. Note that the BrdU staining is both much more uniform and stronger in the wild-type embryo. Neural tube (arrow) remains open in the mutant embryo. Scale bar = 0.1 mm

(E) In vitro proliferation analysis. Embryo fibroblasts were derived from E10.5 embryos of all three genotypes. Identical numbers of cells of each genotype were plated. The growth of these various cultures was measured by counting the total number of cells on each of the indicated days. A representative experiment is shown using fibroblasts of embryos derived from parents with mixed 129 × BL6 backgrounds. Similar results were obtained from three different batches of fibroblasts of each genotype. We noted that $p300^{-/-}$ fibroblasts from 129 inbred embryos exhibited even more severe proliferative defects than fibroblasts shown in this experiment (data not shown).

(Table 2), indicating that compound heterozygous embryos died in utero. Indeed, like both $p300^{-/-}$ and $cbp^{-/-}$ embryos, the compound heterozygous embryos were also severely stunted compared to littermates (Figure 7B) and exhibited open neural tube defects similar to that observed in *p300* or *cbp* homozygous mutants (Figures 7C, 7D, and 3B). Thus, *p300* and *cbp* single-homozygous as well as compound-heterozygous mutants all display similar embryonic phenotypes. Together, these results demonstrate that the combined dose of *p300* and *cbp* is critical for mouse embryonic development. In addition, the results imply that there are important, common embryonic biochemical functions of p300 and CBP.

Discussion

Previous studies in tissue culture cells have suggested that p300 and CBP operate at the end points of signal transduction pathways, which activate specific gene expression programs in response to incoming signals. The gene expression programs thought to be regulated by p300/CBP include those involved in cell differentiation, growth control, and cellular homeostasis. The present work was aimed at testing this notion as well as the potential importance of p300 and CBP function in mouse development. These questions were posed at the hands of discrete loss-of-function mutations in mice.

Four major conclusions emerged from our analysis. First, *p300* and *cbp* are essential genes for mouse embryogenesis. Second, the embryonic phenotypes of $p300^{-/-}$, $cbp^{-/-}$, and compound *p300/cbp* heterozygotes are similar, and, unexpectedly, normal mouse development is sensitive to the *p300* and *cbp* gene dosage. Third and equally surprising was the observation that p300 is essential for normal cell proliferation in vivo and in vitro. Fourth, signaling by retinoic acid is grossly compromised in cells lacking p300, while cAMP (Figure 6) dependent signaling is not.

The early embryonic lethality is a surprise given the presence of normal levels of the highly homologous protein CBP. This result together with the reduced viability of the heterozygous mutants, the nonviability of the compound heterozygotes, and the similarity of the gross anatomical features of these various embryos not only establishes *p300* and *cbp* as essential genes, it also implies that these two proteins exert certain common embryonic survival functions. Since both p300- and CBP-deficient embryos suffered early lethality, this in turn indicates that there is a significant *p300* and *cbp* gene dosage requirement during embryogenesis. Observations made in patients with human RTS syndrome and in adult mouse *cbp* heterozygotes are consistent with this hypothesis (Petrij et al., 1995; Tanaka et al., 1997; T. P. Y. and D. M. L., unpublished data).

The gene dosage effects bear further discussion. Two generic possibilities could explain them. First, one might propose that CBP and p300 can perform numerous common biochemical functions. Given the panoply of different transcription factors with which the two proteins interact and coactivate, it seems fair to argue that p300 and CBP participate in many intracellular signaling pathways. Indeed, the number of pathways might be so large that a drop in the combined level of these proteins of only 0.25-fold (i.e., loss of one allele of *p300*) leaves as many as half of the embryos unable to complete at least

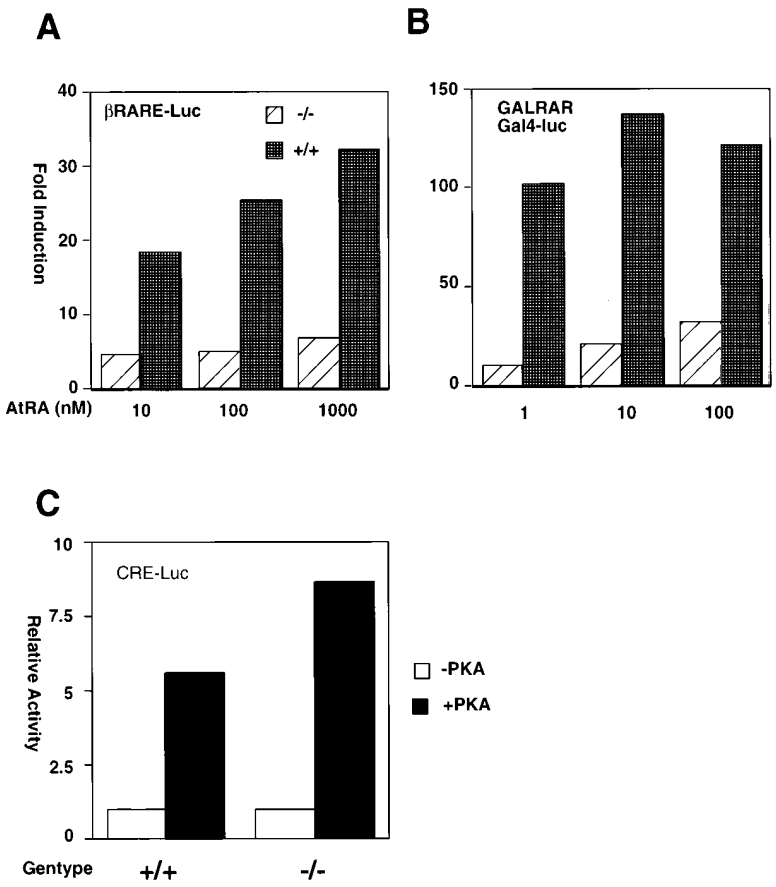

Figure 6. Transcriptional Activity of the Retinoic Acid Receptor but Not of CREB Is Impaired in *p300*$^{-/-}$ Cells

The activity of endogenous RAR (A) and a Gal–RAR fusion protein (B) in response to all *trans*-retinoic acid was measured in *p300* +/+ and −/− primary fibroblasts using bRARE-luciferase and Gal4-luciferase, respectively, as reporters. CREB activity (C) was measured in the absence or presence of the catalytic subunit of protein kinase A (PKA) using somatostatin-CRE-luciferase as a reporter plasmid (this unpublished reagent was the generous gift of Dr. Marc Montminy). The response to all *trans*-retinoic acid (RA) in −/− cells was reduced compared to that in +/+ cells at all concentrations of RA tested. At the same time, PKA-dependent CREB activity was comparable in +/+ and −/− cells.

one function essential for development and survival beyond E9.0–E11.5.

In keeping with our findings and the above-noted models, Rosenfeld and coworkers have provided biochemical evidence from transfection experiments that implies that proper integration of transcription signaling by p300/CBP requires a critical level of these proteins (Kamei et al., 1996). If one considers the evidence from the transfection experiments together with the genetic evidence presented here, one can propose an explanation for the phenomenon of cross-coupling or interference between transcription factors observed in the past by numerous investigators (reviewed in Schule and Evans, 1991). In a model that is relevant to the data presented in this report, an appropriate transcription factor A present at an elevated level engages a number of molecules of p300 and/or CBP, committing them to its coactivation and preventing them from coactivating at least one other specific transcription factor B. Thus, in the absence of its p300 or CBP coactivator, which at that moment in time is committed to cooperating with A, transcription factor B cannot function at a normal rate.

In a second possible explanation for the gene dosage effects, one might argue that despite their high structural similarity and lack of biochemical individuality in transfection experiments, the physiological functions of p300 and CBP do not fully overlap, at least during embryonic development. Thus, a reduction in the dose of one of them cannot be fully compensated by a call on the other to cover the functional deficit.

Not all p300 and CBP functions are similar. We did observe that despite the presence of normal levels of CBP, *p300*$^{-/-}$ fibroblasts were defective in retinoic acid–dependent transcription. By contrast, they displayed normal CREB function, indicating that they have not undergone a general defect in transcription. Consistent with our results, it has been shown by a ribozyme approach using F9 EC cells that p300, but not CBP, is required for retinoic acid signaling (K. Yokoyama, personal communication). These findings, albeit limited in scope, imply that at least in embryonic cells p300 and CBP can also exert certain distinct, nonoverlapping functions.

These data notwithstanding, the nonoverlap of p300 and CBP biochemical functions does not appear to extend to certain major operations for which these proteins are responsible. This is because there were striking similarities in the embryonic phenotypes of *p300*, *cbp*$^{-/-}$, and compound heterozygous knockout embryos (Figures 3 and 7). Hence, these two proteins must also perform a number of operations in common, at least during early embryogenesis.

In a 129/Sv background, a high (but not absolute) degree of embryonic lethality was associated with loss of one *p300* allele. *p300* heterozygotes represent one of the rare cases where haplo-insufficiency of a mammalian gene leads to lethality. Indeed, most heterozygous gene disruption experiments do not result in this effect. A notable exception is the *VEGF* knockout, in which all heterozygous embryos died (Carmeliet et al., 1996; Ferrara et al., 1996). It is important to note that there

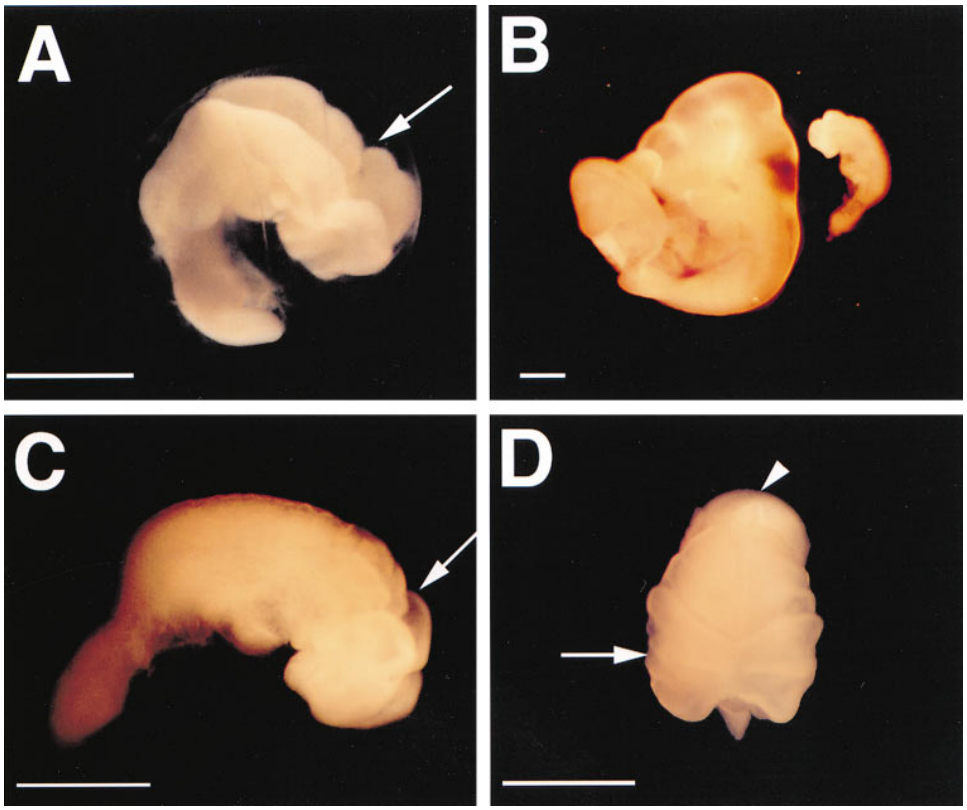

Figure 7. Morphology of $cbp^{-/-}$ and $p300^{+/-}/cbp^{+/-}$ Compound Heterozygous Mutants

(A) A $cbp^{-/-}$ mutant embryo displays open neural tube defects (arrow) similar to those seen in $p300^{-/-}$ embryos (for comparison, see Figure 2B).

(B) A $p300^{+/-}/cbp^{+/-}$ compound heterozygous mutant (smaller embryo) is pictured next to a $p300^{+/+}/cbp^{+/-}$ littermate (left) at E10.5.

(C) Side and dorsal (D) views of the compound heterozygous mutant that exhibits a severe open neural tube defect. Open neural tube (C) and extensive exencephaly (D) are indicated by arrows. Note that the neural tube is fused normally (arrowhead) in the region caudal to the hindbrain, which remains open in the compound heterozygous mutant embryo shown here. Scale bar = 0.8 mm.

appears to be a modifier gene(s) in BL6 mice that suppresses $p300^{+/-}$ lethality. Thus, one or more strain-specific genes can make embryos more (or less) susceptible to a decrease in *p300* or *cbp* gene dosage.

It was remarkable, however, that the embryonic lethality in the 129/Sv background stands in contrast to the lack of overt defects in heterozygotes that survived embryogenesis. Thus, once such +/− embryos have completed gestation, the absolute dependence on *p300* dosage for viability is lost. This result argues that embryogenesis (in the 129/Sv strain reported here) represents a limited period characterized by much greater sensitivity to perturbation in *p300* gene dosage than post-natal life. There may also be sufficient variation in the abundance of p300 at critical times during development so that depending upon whether the protein concentration is sub- or supercritical, the embryo either dies or survives.

p300 and CBP, both E1A binding proteins, have been assumed to function as growth and transformation suppressing elements. The basis for this assumption is that at least part of the E1A stimulation of cell cycle progression is linked to its binding to both nuclear pocket proteins (i.e., Rb family members) and to p300/CBP (reviewed in Moran, 1993). E1A binding releases a negative effect of the pocket protein(s) on cell proliferation. Given this and the fact that E1A binding suppresses p300/CBP transactivating function, it has been widely assumed that p300/CBP, like the pocket proteins, are also active growth suppressers. It was thus unexpected that $p300^{-/-}$ embryos and cultured cells derived from them reveal significant retardation of proliferation. $p300^{-/-}$ embryos were invariably stunted, and, where tested, their tissues revealed reduced DNA synthesis by in situ methodology. These results indicate that p300 is required for growth stimulation and imply that E1A–p300 complexes are even more active in this regard. How these complexes operate to achieve this effect is unclear at present. However, it is worth speculating that there is a link between p300 function and the stable expression of the catalytic subunit of the telomerase gene (Meyerson et al., 1997; Nakamura et al., 1997). Loss of expression of this gene accompanies senescence, and its forced expression overrides the limited lifespan phenotype of primary human (Bodnar et al., 1998). One wonders whether the excessively limited lifespan of $p300^{-/-}$ primary cells is related to premature cessation of telomerase expression and/or failure of its activation. In keeping with the view that p300 is a growth-promoting element is the discovery of spontaneously occurring

human p300 fusion proteins that appear to contribute to leukemia development (Ida et al., 1997). Alternatively, p300 might be a cellular protein endowed with both growth-suppressing and -stimulating activities.

The early death of *p300*$^{-/-}$ mutant embryos has prevented us from examining the behavior of several important differentiation programs, such as skeletal muscle differentiation, that appear to be dependent on p300 and/or CBP based upon evidence obtained in cultured cells (Eckner et al., 1996a; Puri et al., 1997). The present study, however, supports the view, which arose from analysis of the results of studies in tissue culture cells, that p300 participates in certain cellular differentiation programs. The heart is the first organ of a mouse embryo to achieve full functionality. Inspection of this organ in *p300*$^{-/-}$ embryos revealed defects of cardiac muscle differentiation and in trabeculation. Expression of the structural proteins myosin and α-actinin was clearly reduced in mutant hearts compared to the wild-type hearts of littermates.

Expression of cardiac muscle structural proteins depends on members of the MEF2 transcription factor family (Lin et al., 1997). Although it is formally possible that the heart defect is secondary to a developmental delay observed in *p300*$^{-/-}$ mutant embryos, we showed earlier that MEF2 proteins, which also regulate cardiac development, bind to p300 and CBP in vivo (Eckner et al., 1996a). Thus, we speculate that the impaired activity of MEF2 proteins in the absence of p300 underlies the observed defects in the expression of certain myocardial contractile proteins. Such a conclusion is supported by a recent report showing that p300 stimulates cell type–specific gene expression in cardiac myocytes (Hasegawa et al., 1997). Taken together, our results argue that p300 is required for proper heart development. The cardiac defects in *p300*$^{-/-}$ embryos may constitute a major reason for the lethality observed between E9.0 and E11.5.

All *p300*$^{-/-}$ embryos displayed an open neural tube defect. Although many murine mutations have been shown to affect tube closure, the phenotype of *p300*$^{-/-}$ mutants shows some similarities to that of a mouse *twist* mutant, which also dies at ~E10.5 (Chen and Behringer, 1995). Interestingly, a mutation of the *Drosophila p300/cbp* homolog *dcbp* affects the normal expression of *Drosophila twist* due to a defect in the transcription activity of *dorsal* (Akimaru et al., 1997). *Dorsal* activates *twist* and, like its mammalian relative NF-kB, requires a p300/CBP family member to function in transcription (Gerritsen et al., 1997; Perkins et al., 1997). Thus, it is possible that the neural tube defect of *p300*$^{-/-}$ embryos is due to a defect in murine *twist*. A defect in other p300-dependent transcription factors required for proper neural tube morphogenesis, such as AP-2 and PAX-3, may also contribute to the neural tube defect (Epstein et al., 1991; Schorle et al., 1996).

The retinoic acid–dependent transcription defect observed in *p300*$^{-/-}$ cells, while distinct, was not complete. Moreover, the same cells displayed certain normal transcriptional responses (such as that mediated by CREB) in which p300 and/or CBP have long been assumed to participate. Hence, these cells are not generally defective in polymerase II transcriptional responses.

We also hypothesize that the severe developmental phenotype observed in the *p300*$^{-/-}$, *cbp*$^{-/-}$, and compound heterozygous embryos reflects a defect not in a single signaling response but rather in the simultaneous coordination of multiple signaling events, e.g., in cross-coupling. It is also possible that the transcriptional deficits associated with the lack of p300 are only incompletely revealed in standard transfection assays. For example, p300 can function as a histone acetyltransferase. Conceivably, its activity in this regard only becomes essential in the context of a physiologically folded chromatin structure, which is not faithfully reproduced in transiently transfected model reporter plasmids (Dillon and Grosveld, 1993).

Given the observations reported here, a major goal will now be to understand the biochemical basis for *p300/cbp* dosage dependence and p300 cellular proliferation control. Detailed analysis of selected p300 mutant genes is likely to provide significant insights into these mechanisms. Understanding them should in turn shed light on how a critical number of molecules of p300 and CBP connect so many seemingly disparate and highly complex transcriptional functions to events that are essential for embryonic growth, organ development, and cellular homeostasis.

Experimental Procedures

Generation of ES Cells Heterozygous for *p300*

An 129 mouse genomic λ EMBL3 phage library (gift of Dr. Gerard Grosveld) was screened with a probe derived from the 5′ end of the murine *p300* cDNA. The locations of exons were mapped by Southern blotting and PCR analyses. The precise exon–intron boundaries were determined by sequencing. The targeting vector was constructed with an 11 kb Asp-718 genomic fragment. First, a ca. 2 kb genomic BstXI–BglI fragment encompassing two complete exons and a part of another two exons was deleted and replaced by a BamHI linker. The BstXI and BglI sites used are both located within exons. The deleted exons encoded the first Cys/His-rich region. Subsequently, a PGK-*neo* cassette was cloned as a BglII fragment into the newly inserted BamHI site. Finally, a SalI fragment containing the negative selection marker PGK− (Clarke et al., 1992) was inserted at the 5′ end of the 11 kb fragment. J-1 ES cells (Li et al., 1992) were electroporated with the targeting plasmid linearized by HpaI. From 140 analyzed ES cell colonies surviving selection with G418 and FIAU, 3 contained a correctly targeted allele. These cells were individually injected into blastocysts derived from C57Bl/6 mice. Two of the three ES cell clones gave rise to chimeric mice that transmitted the targeted allele to the germline.

Histological Analysis

Embryos of various stage were isolated and fixed in either Bouin's solution or 4% paraformaldehyde for 2–4 hr at room temperature, dehydrated in ethanol series, cleared in xylene, and embedded in paraffin. Sections were cut at 6–7 μm and either stained with hematoxylin and eosin or processed for immunostaining.

BrdU Labeling and Immunohistochemistry

E9.5 embryos were labeled with BrdU by injecting pregnant mice with 0.5 ml of BrdU/PBS solution (3 mg/ml). The mice were sacrificed 1.5 hr later, and embryos were isolated and processed as described above. For immunohistochemistry, the proper sections were rehydrated, partially digested with proteinase (25 μg/ml, bacterial type XXIV, Sigma) and then reacted with specific antibody. The detection of BrdU incorporation was performed following the manufacturer's instructions (Cell Proliferation Kit, Boehringer Mannheim). For myosin heavy chain staining, monoclonal antibody MF20 was used, and the detection phase was carried out using the ABC kit (AP Kit, Vector).

Preparation of Mouse Fibroblasts and Analysis

Embryos showing a clearly visible heartbeat were isolated at E10.5, decapitated, and dissociated by gentle pippeting and trypsin digestion. The dissociated fibroblasts were allowed to settle and then cultured in standard DMEM containing 10% serum (Fetal Clone I, Hyclone). The viability of fibroblasts was comparable among all three genotypes after explantation as judged by trypan blue exclusion assays. For growth curve analysis, 10^4 of cells of each genotype were plated in a 12-well culture plate (Costar), and the cell number was counted at the indicated time.

Transfection and Plasmids

Transfection was performed using Lipofectamine (GIBCO BRL). Briefly, primary MEF cells derived from embryos were transfected with the indicated DNA for 2.5–3 hr. The lipofectamine/DNA mix was then replaced with fresh medium. For analysis of a retinoic acid response, all *trans*-retinoic acid was added to the medium one day after transfection. Transfected cells were harvested 24–36 hr later and assayed for luciferase activity. β-galactosidase activity was measured by a chemiluminescent assay (Tropix) and used as the transfection control. Gal-RAR and the reporter system have been described (Forman et al., 1995). CRE-Luc (somatostatin-CRE) is a gift of Dr. Marc Montminy.

Genotyping the Mice

Tail or yolk sac DNA was prepared by a standard method. The genotype of the animals was determined either by Southern analysis with a specific probe (described in Figure 2) or by polymerase chain reaction (PCR) using specific primers to amplify the *neo* gene and a specific exon that is deleted in the targeted allele (sequences of the primers available upon request).

Western Analysis

Whole cell extracts were prepared from embryo fibroblasts, fractionated in SDS gels, and transferred to nitrocellulose membranes. p300 and CBP were detected by staining with p300-specific (RW128) or CBP-specific monoclonal antibody (AC26). p400 was detected with another p300/CBP monoclonal antibody, RW144. Staining was visualized by ECL method (Amersham).

In Situ Hybridization

Balb/c mice were mated overnight, and the morning of vaginal plug detection was defined as 0.5 days of gestation. For in situ hybridization, embryos of various stages of mouse development were embedded in Tissue-Tek, frozen on the surface of liquid nitrogen, and stored at −70°C prior to use. Sectioning, postfixation, preparation of the single-stranded probe, and hybridization were performed as described previously (Millauer et al., 1993). The *p300* DNA fragment used as hybridization probe corresponds to amino acids 39–572 of murine p300 (sequence available upon request). Briefly, RNA transcripts were synthesized from the linearized plasmid using T3- or T7-RNA-Polymerase (Boehringer) and the DNA was degraded using DNase (RNase-free preparation, Boehringer). The RNA transcripts were used for random-primed cDNA synthesis with [^{35}S]-α-dATP (Amersham) by reverse transcription with MMLV Reverse Transcriptase (BRL), resulting in small cDNA transcripts with a size of about 100 bp. After hydrolysis of the RNA, the probe was purified by Sephadex-G50 column chromatography. Sections 10 μm thick were incubated overnight with the [^{35}S]-cDNA probe (final concentration 2×10^4 cpm per μl) at 52°C in a buffer containing 50% formamide, 300 mM NaCl, 10 mM Tris-HCl, 10 mM $NaPO_4$ (pH 6.8), 5 mM EDTA, 0.02% Ficoll 400, 0.02% Polyvinylpyrrolidone, 0.02% BSA, 1 mg ml^{-1} yeast RNA, 10% dextran sulfate, and 10 mM DTT. Posthybridization washing was performed at high stringency (50% formamide, 300 mM NaCl, 10 mM Tris-HCl, 10 mM $NaPO_4$ [pH 6.8], 5 mM EDTA, and 10 mM DTT at 52°C). Slides were coated with Kodak NTB2 film emulsion and exposed for approximately 7 days.

Acknowledgments

We thank Dr. Gerard Grosveld for the 129 genomic library; Dr. Hein te Riele for PGK-*neo* and PGK-*tk* selection plasmids; Dr. Marc Montminy for a somatostatin-luciferase reporter plasmid; Dr. Cheng Lai, Dr. Jay Schnider, Elizabeth Oldread, Caroline Schnell, and Hong Yang for technical help; and Dr. Arlene Sharpe for advice on ES cell growth. We wish to thank Drs. Henry Sucov and Pamela Mitchell for their invaluable advice during our analyses of murine embryogenesis. We also thank our laboratory colleagues for many helpful and enlightening discussions. This work was supported by grants from the National Institutes of Health (NCI) and from the Novartis Drug Discovery Program (to D. M. L.). Some of this work was also supported by a START grant from the Swiss National Science Foundation to R. E. T.-P. Y. was supported by a fellowship from the Damon Runyan-Walter Winchill Cancer Research Fund (DRG1359), and M. F. was supported by a fellowship from the Deutsche Forschungsgemeinschaft.

Received January 21, 1998; revised March 19, 1998.

References

Akimaru, H., Hou, D., and Ishii, S. (1997). *Drosophila* CBP is required for dorsal-dependent twist gene expression. Nat. Genet. *17*, 211–214.

Arany, Z., Sellers, W.R., Livingston, D.M., and Eckner, R. (1994). E1A-associated p300 and CREB-associated CBP belong to a conserved family of coactivators. Cell *77*, 799–800.

Avantaggiati, M.L., Ogryzko, V., Gardner, K., Giordano, A., Levine, A.S., and Kelly, K. (1997). Recruitment of p300/CBP in p53-dependent signal pathways. Cell *89*, 1175–1184.

Bannister, A.J., and Kouzarides, T. (1996). The CBP co-activator is a histone acetyltransferase. Nature *384*, 641–643.

Bodnar, A.G., Ouellette, M., Frolkis, M., Holt, S.E., Chiu, C., Morin, G.B., Harley, C.B., Shay, J.W., Lichtsteiner, S., and Wright, W.E. (1998). Extension of life-span by introduction of telomerase into normal human cells. Science *279*, 349–352.

Borrow, J., Stanton, V.J., Andresen, J.M., Becher, R., Behm, F.G., Chaganti, R.S., Civin, C.I., Disteche, C., Dube, I., Frischauf, A.M., et al. (1996). The translocation t(8;16)(p11;p13) of acute myeloid leukaemia fuses a putative acetyltransferase to the CREB-binding protein. Nat. Genet. *14*, 33–41.

Carmeliet, P., Ferreira, V., Breier, G., Pollefeyt, S., Kieckens, L., Gertsenstein, M., Fahrig, M., Vandenhoeck, A., Harpal, K., Eberhardt, C., et al. (1996). Abnormal blood vessel development and lethality in embryos lacking a single VEGF allele. Nature *380*, 435–439.

Chen, Z.F., and Behringer, R.R. (1995). twist is required in head mesenchyme for cranial neural tube morphogenesis. Genes Dev. *9*, 686–699.

Chen, H., Lin, R.J., Schiltz, R.L., Chakravarti, D., Nash, A., Nagy, L., Privalsky, M.L., Nakatani, Y., and Evans, R.M. (1997). Nuclear receptor coactivator ACTR is a novel histone acetyltransferase and forms a multimeric activation complex with P/CAF and CBP/p300. Cell *90*, 569–580.

Chrivia, J.C., Kwok, R.P., Lamb, N., Hagiwara, M., Montminy, M.R., and Goodman, R.H. (1993). Phosphorylated CREB binds specifically to the nuclear protein. Nature *365*, 855–859.

Clarke, A.R., Maandag, E.R., Roon, M.V., Lugt, N., Valk, M., Hooper, M.L., Berns, A., and Riele, H.T. (1992). Requirement for a functional RB-1 gene in murine development. Nature *359*, 328–330.

Dillon, N., and Grosveld, F. (1993). Transcriptional regulation of multigene loci: multilevel control. Trends Genet. *9*, 134–137.

Eckner, R., Ewen, M.E., Newsome, D., Gerdes, M., DeCaprio, J.A., Lawrence, J.B., and Livingston, D.M. (1994). Molecular cloning and functional analysis of the adenovirus E1A-associated 300-KD protein (p300) reveals a protein with properties of a transcriptional adaptor. Genes Dev. *7*, 869–884.

Eckner, R., Yao, T.P., Oldread, E., and Livingston, D.M. (1996a). Interaction and functional collaboration of p300/CBP and bHLH proteins in muscle and B-cell differentiation. Genes Dev *10*, 2478–2490.

Eckner, R., Ludlow, J.W., Lill, N.L., Oldread, E., Arany, Z., Modjtahedi, N., DeCaprio, J.A., Livingston, D.M., and Morgan, J.A. (1996b). Association of p300 and CBP with simian virus 40 large T antigen. Mol. Cell. Biol. *16*, 3454–3464.

Epstein, D.J., Vekemans, M., and Gross, P. (1991). *splotch* (*Sp^{2H}*), a mutation affecting development of the mouse neural tube, shows a deletion within the paired homeodomain of Pax-3. Cell *67*, 767–774.

Ferrara, N., Carver, M.K., Chen, H., Dowd, M., Lu, L., O'Shea, K.S., Powell, B.L., Hillan, K.J., and Moore, M.W. (1996). Heterozygous embryonic lethality induced by targeted inactivation of the VEGF gene. Nature *380*, 439–442.

Forman, B.M., Umesono, K., Chen, J., and Evans, R.M. (1995). Unique response pathways are established by allosteric interactions among nuclear hormone receptors. Cell *81*, 541–550.

Gerritsen, M.E., Williams, A.J., Neish, A.S., Moore, S., Shi, Y., and Collins, T. (1997). CREB-binding protein/p300 are transcriptional coactivators of p65. Proc. Natl. Acad. Sci. USA *94*, 2927–2932.

Grunstein, M. (1997). Histone acetylation in chromatin structure and transcription. Nature *389*, 349–352.

Gu, W., and Roeder, R.G. (1997). Activation of p53 sequence-specific DNA binding by acetylation of the p53 C-terminal domain. Cell *90*, 595–606.

Gu, W., Shi, X.L., and Roeder, R.G. (1997). Synergistic activation of transcription by CBP and p53. Nature *387*, 819–823.

Hanstein, B., Eckner, R., DiRenzo, J., Halachmi, S., Liu, H., Searcy, B., Kurokawa, R., and Brown, M. (1996). p300 is a component of an estrogen receptor coactivator complex. Proc. Natl. Acad. Sci. USA *93*, 11540–11545.

Hasegawa, K., Meyers, M.B., and Kitsis, R.N. (1997). Transcriptional coactivator p300 stimulates cell type–specific gene expression in cardiac myocytes. J. Biol. Chem. *272*, 20049–20054.

Howe, J.A., Mymryk, J.S., Egan, C., Branton, P.E., and Bayley, S.T. (1990). Retinoblastoma growth suppressor and a 300-kDa protein appear to regulate cellular DNA synthesis. Proc. Natl. Acad. Sci. USA *87*, 5883–5887.

Ida, K., Kitabayashi, I., Taki, T., Taniwaki, M., Noro, K., Yamamoto, M., Ohki, M., and Hayashi, Y. (1997). Adenoviral E1A-associated protein p300 is involved in acute myeloid leukemia with t(11;22). Blood *90*, 4699–4704.

Kamei, Y., Xu, L., Heinzel, T., Torchia, J., Kurokawa, R., Gloss, B., Lin, S., Heyman, R.A., Rose, D.W., Glass, C.K., and Rosenfeld, M.G. (1996). A CBP integrator complex mediates transcriptional activation and AP-1 inhibition by nuclear receptors. Cell *85*, 403–414.

Li, E., Bestor, T.H., and Jaenisch, R. (1992). Targeted mutation of the DNA methyltransferase gene results in embryonic lethality. Cell *69*, 915–926.

Lill, N.L., Grossman, S.R., Ginsberg, D., DeCaprio, J., and Livingston, D.M. (1997). Binding and modulation of p53 by p300/CBP coactivators. Nature *387*, 823–827.

Lin, Q., Schwarz, J., Bucana, C., and Olson, E.N. (1997). Control of mouse cardiac morphogenesis and myogenesis by transcription factor MEF2C. Science *276*, 1404–1407.

Meyerson, M., Counter, C.M., Eaton, E.N., Ellisen, L.W., Steiner, P., Caddle, S.D., Ziaugra, L., Beijersbergen, R.L., Davidoff, M.J., Liu, Q., et al. (1997). *hEST2*, the putative human telomerase catalytic subunit gene, is up-regulated in tumor cells and during immortalization. Cell *90*, 785–795.

Millauer, B., Wizigmann-Voss, S., Schnürch, H., Martinez, R., Møller, N.P.H., Risau, W., and Ullrich, A. (1993). High affinity VEGF binding and developmental expression suggest FLK-1 as a major regulator of vasculogenesis and angiogenesis. Cell *72*, 835–846.

Molkentin, J.D., Black, B.L., Martin, J.F., and Olson, E.N. (1995). Cooperative activation of muscle gene expression by MEF2 and myogenic bHLH proteins. Cell *83*, 1125–1136.

Moran, E. (1993). DNA tumor virus transforming proteins and the cell cycle. Curr. Opin. Genet. Dev. *3*, 63–70.

Nakajima, T., Uchida, C., Anderson, S.F., Lee, C.G., Hurwitz, J., Parvin, J.D., and Montminy, M. (1997a). RNA helicase A mediates association of CBP with RNA polymerase II. Cell *90*, 1107–1112.

Nakajima, T., Uchida, C., Anderson, S.F., Parvin, J.D., and Montminy, M. (1997b). Analysis of a cAMP-responsive activator reveals a two-component mechanism for transcriptional induction via signal-dependent factors. Genes Dev. *11*, 738–747.

Nakamura, T.M., Morin, G.B., Chapman, K.B., Weinrich, S.L., Andrews, W.H., Lingner, J., Harley, C.B., and Cech, T.R. (1997). Telomerase catalytic subunit homologs from fission yeast and human [see comments]. Science *277*, 955–959.

Nevins, J.R. (1992). E2F: a link between the Rb tumor suppressor protein and viral oncoproteins. Science *258*, 424–429.

Oelgeschlager, M., Janknecht, R., Krieg, J., Schreek, S., and Luscher, B. (1996). Interaction of the co-activator CBP with Myb proteins: effects on Myb-specific transactivation and on the cooperativity with NF-M. EMBO J. *15*, 2771–2780.

Ogryzko, V.V., Schiltz, R.L., Russanova, V., Howard, B.H., and Nakatani, Y. (1996). The transcriptional coactivators p300 and CBP are histone acetyltransferases. Cell *87*, 953–959.

Parker, D., Ferreri, K., Nakajima, T., LaMorte, V.J., Evans, R., Koerber, S.C., Hoeger, C., and Montminy, M.R. (1996). Phosphorylation of CREB at Ser-133 induces complex formation with CREB-binding protein via a direct mechanism. Mol. Cell. Biol. *16*, 694–703.

Perkins, N.D., Felzien, L.K., Betts, J.C., Leung, K., Beach, D.H., and Nabel, G.J. (1997). Regulation of NF-kappaB by cyclin-dependent kinases associated with the p300 coactivator. Science *275*, 523–527.

Petrij, F., Giles, R.H., Dauwerse, H.G., Saris, J.J., Hennekam, R.C., Masuno, M., Tommerup, N., van Ommen, O.G., Goodman, R.H., Peters, D.J., et al. (1995). Rubinstein-Taybi syndrome caused by mutations in the transcriptional co-activator CBP. Nature *376*, 348–351.

Puri, P.L., Avantaggiati, M.L., Balsano, C., Sang, N., Graessmann, A., Giordano, A., and Levrero, M. (1997). p300 is required for MyoD-dependent cell cycle arrest and muscle-specific gene transcription. Embo J *16*, 369–83.

Sartorelli, V., Huang, J., Hamamori, Y., and Kedes, L. (1997). Molecular mechanisms of myogenic coactivation by p300: direct interaction with the activation domain of MyoD and with the MADS box of MEF2C. Mol. Cell. Biol. *17*, 1010–1026.

Schorle, H., Meier, P., Buchert, M., Jaenisch, R., and Mitchell, P.J. (1996). Transcription factor AP-2 essential for cranial closure and craniofacial development. Nature *381*, 235–238.

Schule, R., and Evans, R.M. (1991). Cross-coupling of signal transduction pathways: zinc finger meets leucine zipper. Trends Genet. *7*, 377–381.

Shikama, N., Lyon, L., and La Thangue, N.B. (1997). The p300/CBP family: integrating signals with transcription factors and chromatin. Trends Cell Biol. *7*, 230–236.

Smith, C.L., Onate, S.A., Tsai, M.J., and O'Malley, B.W. (1996). CREB binding protein acts synergistically with steroid receptor coactivator-1 to enhance steroid receptor–dependent transcription. Proc. Natl. Acad. Sci. USA *93*, 8884–8888.

Sobulo, O.M., Borrow, J., Tomek, R., Reshmi, S., Harden, A., Schlegelberger, B., Housman, D., Doggett, N.A., Rowley, J.D., and Zeleznik, L.N. (1997). MLL is fused to CBP, a histone acetyltransferase, in therapy-related acute myeloid leukemia with a t(11;16)(q23;p13.3). Proc. Natl. Acad. Sci. USA *94*, 8732–8737.

Tanaka, Y., Naruse, I., Maekawa, T., Masuya, H., Shiroishi, T., and Ishii, S. (1997). Abnormal skeletal patterning in embryos lacking a single Cbp allele: a partial similarity with Rubinstein-Taybi syndrome. Proc. Natl. Acad. Sci. USA *94*, 10215–10220.

Torchia, J., Rose, D.W., Inostroza, J., Kamei, Y., Westin, S., Glass, C.K., and Rosenfeld, M.G. (1997). The transcriptional co-activator p/CIP binds CBP and mediates nuclear-receptor function. Nature *387*, 677–684.

Wade, P.A., Pruss, D., and Wolffe, A.P. (1997). Histone acetylation: chromatin in action. Trends Biochem. Sci. *22*, 128–132.

Whyte, P., Williamson, N.M., and Harlow, E. (1989). Cellular targets for transformation by the adenovirus E1A. Cell *56*, 67–75.

Yang, X.J., Ogryzko, V.V., Nishikawa, J., Howard, B.H., and Nakatani, Y. (1996). A p300/CBP-associated factor that competes with the adenoviral oncoprotein E1A. Nature *382*, 319–324.

Yao, T.P., Ku, G., Zhou, N., Scully, R., and Livingston, D.M. (1996). The nuclear hormone receptor coactivator SRC-1 is a specific target of p300. Proc. Natl. Acad. Sci. USA *93*, 10626–10631.